

ON LONG-TERM SPACE-CHARGE TRACKING SIMULATION*

J. Qiang[†], LBNL, Berkeley, USA

Abstract

The nonlinear space-charge effects in high intensity accelerator can degrade beam quality and cause particle losses. Self-consistent macroparticle tracking simulations have been widely used to study these space-charge effects. However, it is computationally challenging for long-term tracking simulation of these effects. In this paper, we study a fully symplectic self-consistent particle-in-cell model and numerical methods to mitigate numerical emittance growth. We also discuss about a fast alternative frozen space-charge model that has a potential to improve computational speed significantly.

INTRODUCTION

The nonlinear space-charge effects present strong limit on beam intensity in high intensity/high brightness accelerators by causing beam emittance growth, halo formation, and even particle losses. Self-consistent macroparticle simulations have been widely used to study these space-charge effects in the accelerator community [1–13]. In some applications, especially in high intensity synchrotron, one has to track the beam for many turns. It becomes computationally challenging for the long-term space charge tracking simulation since on one hand one needs to ensure the accuracy of the simulation results to avoid numerical artifacts, and on the other hand, one would like to reduce the computing time for fast physics applications.

The charged particle motion inside an accelerator follows classical Hamiltonian dynamics and satisfies the symplectic conditions. It is desirable to preserve the symplectic conditions in the long-term numerical tracking simulation too. Violating the symplectic conditions in numerical integration results in unphysical results [14, 15]. A gridless symplectic space-charge tracking model and a symplectic particle-in-cell (PIC) model were proposed in recent studies [16, 17].

Even with the use of the symplectic space-charge model, there still exists artificial emittance growth caused by the smaller number of macroparticles used in the simulation compared with the real number of particles inside the beam. In this study, we proposed a threshold filtering method to mitigate the numerical emittance growth. In order to improve computational speed in long-term tracking simulation, we also explored a frozen space-charge model in the simulation.

* Work supported by the U.S. Department of Energy under Contract No. DE-AC02-05CH11231.

[†] jqiang@lbl.gov

SYMPLECTIC PARTICLE-IN-CELL MODEL

In the symplectic particle-in-cell (PIC) model, a single step macroparticle advance can be given as:

$$\begin{aligned}\zeta(\tau) &= \mathcal{M}(\tau)\zeta(0) \\ &= \mathcal{M}_1(\tau/2)\mathcal{M}_2(\tau)\mathcal{M}_1(\tau/2)\zeta(0) + O(\tau^3)\end{aligned}\quad (1)$$

where the transfer map \mathcal{M}_1 corresponds to the single particle Hamiltonian including external fields and the transfer map \mathcal{M}_2 corresponds to space-charge potential from multi-particle Coulomb interactions. This numerical integrator Eq. 1 will be symplectic if both the transfer map \mathcal{M}_1 and the transfer map \mathcal{M}_2 are symplectic. For a coasting beam inside a rectangular conducting pipe, the space-charge potential can be obtained from the solution of the Poisson equation using a spectral method [17]. The one-step symplectic transfer map \mathcal{M}_2 of the particle i for the space-charge Hamiltonian is given as:

$$\begin{aligned}p_{xi}(\tau) &= p_{xi}(0) - \tau 4\pi K \sum_I \sum_J \frac{\partial S(x_I - x_i)}{\partial x_i} \times \\ &S(y_J - y_i)\phi(x_I, y_J) \\ p_{yi}(\tau) &= p_{yi}(0) - \tau 4\pi K \sum_I \sum_J S(x_I - x_i) \times \\ &\frac{\partial S(y_J - y_i)}{\partial y_i} \phi(x_I, y_J)\end{aligned}\quad (2)$$

where both p_{xi} and p_{yi} are normalized by the reference particle momentum p_0 , $K = qI/(2\pi\epsilon_0 p_0 v_0^2 \gamma_0^2)$ is the generalized perveance, I is the beam current, ϵ_0 is the permittivity of vacuum, p_0 is the momentum of the reference particle, v_0 is the speed of the reference particle, γ_0 is the relativistic factor of the reference particle, $S(x)$ is the unitless shape function (also called deposition function in the PIC model), and the ϕ is given as:

$$\begin{aligned}\phi(x_I, y_J) &= \frac{4}{ab} \sum_{l=1}^{N_l} \sum_{m=1}^{N_m} \frac{1}{\gamma_{lm}^2} \sum_{I'} \sum_{J'} \bar{\rho}(x_{I'}, y_{J'}) \times \\ &\sin(\alpha_l x_{I'}) \sin(\beta_m y_{J'}) \sin(\alpha_l x_I) \sin(\beta_m y_J)\end{aligned}$$

where the integers I, J, I' , and J' denote the two dimensional computational grid index, and the summations with respect to those indices are limited to the range of a few local grid points depending on the specific deposition function. The density related function $\bar{\rho}(x_{I'}, y_{J'})$ on the grid can be obtained from:

$$\bar{\rho}(x_{I'}, y_{J'}) = \frac{1}{N_p} \sum_{j=1}^{N_p} S(x_{I'} - x_j) S(y_{J'} - y_j), \quad (4)$$

In the PIC literature, some compact function such as linear function and quadratic function is used in the simulation. For

Content from this work may be used under the terms of the CC BY 3.0 licence (© 2018). Any distribution of this work must maintain attribution to the author(s), title of the work, publisher, and DOI.

example, a quadratic shape function can be written as [18, 19]:

$$S(x_I - x_i) = \begin{cases} \frac{3}{4} - \left(\frac{x_i - x_I}{\Delta x}\right)^2, & |x_i - x_I| \leq \Delta x/2 \\ \frac{1}{2} \left(\frac{3}{2} - \frac{|x_i - x_I|}{\Delta x}\right)^2, & \Delta x/2 < |x_i - x_I| \leq 3/2\Delta x \\ 0 & \text{otherwise} \end{cases}$$

$$\frac{\partial S(x_I - x_i)}{\partial x_i} = \begin{cases} -2\left(\frac{x_i - x_I}{\Delta x}\right)/\Delta x, & |x_i - x_I| \leq \Delta x/2 \\ \left(-\frac{3}{2} + \frac{(x_i - x_I)}{\Delta x}\right)/\Delta x, & \Delta x/2 < |x_i - x_I| \leq 3/2\Delta x, x_i > x_I \\ \left(\frac{3}{2} + \frac{(x_i - x_I)}{\Delta x}\right)/\Delta x, & \Delta x/2 < |x_i - x_I| \leq 3/2\Delta x, x_i \leq x_I \\ 0 & \text{otherwise} \end{cases}$$

The same shape function and its derivative can be applied to the y dimension.

Using the symplectic transfer map \mathcal{M}_1 for the single particle Hamiltonian including external fields from a magnetic optics code [20–22] and the transfer map \mathcal{M}_2 for space-charge Hamiltonian, one obtains a symplectic PIC model including the self-consistent space-charge effects.

As a test of the above symplectic PIC model, we compared this model with another gridless symplectic space-charge model and a nonsymplectic PIC solver. Figure 1 shows the emittance growth evolution through a FODO lattice with 85 degree zero current phase advance and 42 degree depressed phase advance from these three models. These simulations

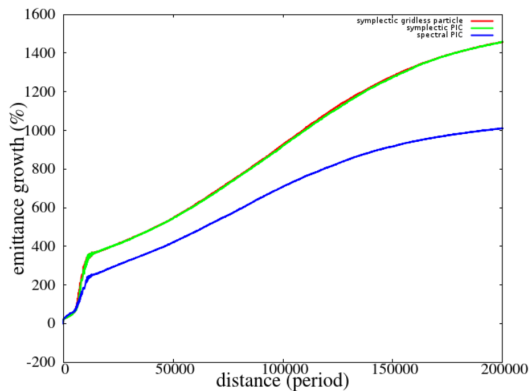


Figure 1: 4D emittance growth in a FODO lattice using the symplectic gridless model, the symplectic PIC model and the non-symplectic PIC model.

used about 50,000 macroparticles and 15×15 modes in the spectral Poisson solver. It is seen that the symplectic PIC model and the symplectic gridless particle model agrees with each other very well. The nonsymplectic spectral PIC model yields significantly smaller emittance growth than those from the two symplectic methods, which might result from the numerical damping effects in the nonsymplectic integrator. The fast emittance growth within the first 20,000 periods is caused by the space-charge driven 4th order collective instability. The slow emittance growth after 20,000 periods might be due to numerical collisional effects.

MITIGATION OF NUMERICAL NOISE INDUCED EMITTANCE GROWTH

In long-term macroparticle space-charge tracking simulation, even with the use of self-consistent symplectic space-charge model, there still exists numerical emittance growth. Figure 2 shows the four dimensional emittance

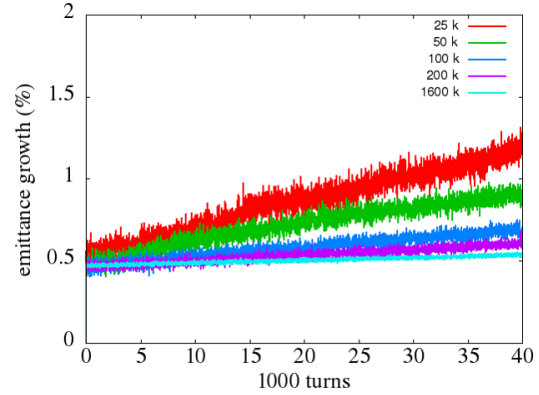


Figure 2: 4D emittance growth in a FODO lattice using several numbers of macroparticles in the simulation.

growth $\left(\frac{\epsilon_x}{\epsilon_{x0}} \frac{\epsilon_y}{\epsilon_{y0}} - 1\right)\%$ evolution of a 1 GeV, 30A current proton beam through 40,000 turns of a lattice that consists of 10 FODO elements (zero current tune 2.417) with 25,000, 50,000, 100,000, 200,000, and 1.6 million macroparticles and 64×64 modes. The initial 0.5% jump of emittance growth is due to charge redistribution to match into the lattice. It is seen that with the increase of the number of macroparticles, the emittance growth becomes smaller. With the use of 1.6 million macroparticles, there is little emittance growth which is expected in this linear lattice. The extra numerical emittance growth with small number of macroparticles is due to numerical collisional effect. This numerical collisional effect is caused by the artificially increased charge per macroparticle used in the simulation since the number of macroparticles is much less than the real number of protons inside the beam. The small number of macroparticles enhances the fluctuation of charge density distribution and induces numerical emittance growth.

The numerical fluctuation can be smoothed out by using a numerical filter in the frequency domain. Instead of using a standard cut-off method beyond some frequencies, we proposed using an amplitude threshold method to remove unwanted high frequency noise. In this method, the mode with an amplitude below a threshold value multiplying the maximum amplitude in the density spectral distribution is removed from the distribution. The advantage of this method is instead of removing all high frequency modes, it will keep the high frequency modes with sufficiently large amplitudes. These high frequency modes can represent some real physics structures inside the beam. Figure 3 shows the spectral amplitude of a 2D Gaussian density distribution without and with 1% threshold filter. The standard cut-off filter with 16×16 and 32×32 modes are also indicated in above plot.

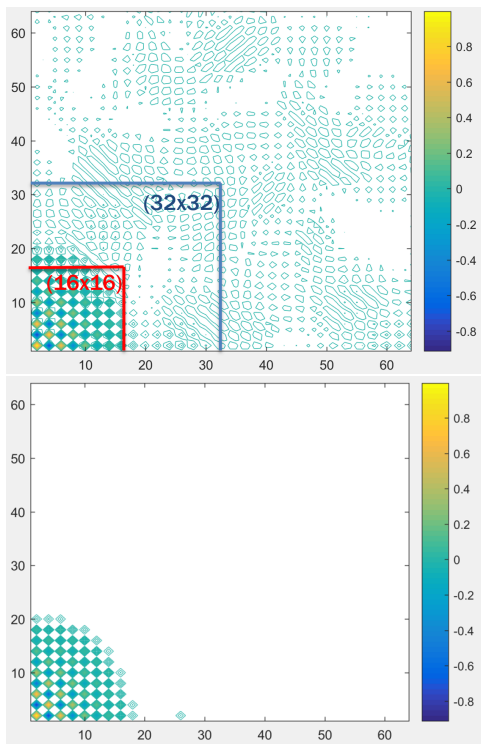


Figure 3: Spectral amplitude of a 2D Gaussian distribution without (top) and with 1% threshold filter.

Most high frequency noise is removed in this distribution by using the threshold filtering method.

As a test of the threshold filtering method, we reran the above space-charge long-term simulation using 0 (no filtering), 0.005, 0.1 and 0.05 threshold filtering the charge density distribution during the simulation and 25,000 macroparticles. Here, the larger threshold value, the less number of modes will be included in the simulation. It is seen that

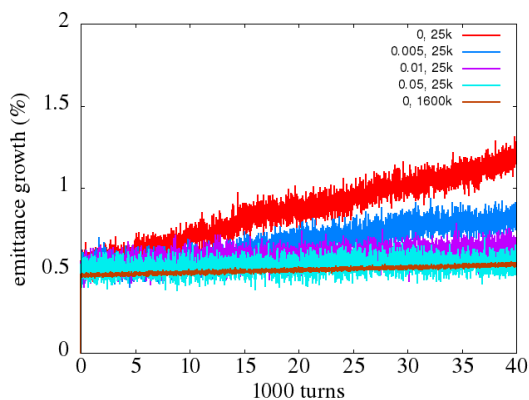


Figure 4: 4D emittance growth with 0 (no filtering) with 0.005, 0.01 and 0.05 threshold filtering of charge density distribution using 25k macroparticles and 0 filtering using 1600k macroparticles.

without numerical threshold filtering, there is significant emittance growth after 40,000 turns. With 0.05 threshold filtering, there is little emittance growth, which is consistent

with the expected physics emittance growth as seen by using 1600k macroparticles without filtering.

In order to improve the computational speed, we explored a frozen space-charge model during the simulation. Here, instead of self-consistently updating the space-charge Poisson solver every time step, after some initial time steps, we store the solutions of the space-charge fields along the lattice and reuse those stored space-charge fields for the following long-term simulation. This model assumes that after some steps, the charge density distribution of the beam attains stable solutions and will not vary significantly from turn to turn. Figure 5 shows the total 4D emittance growth evolution

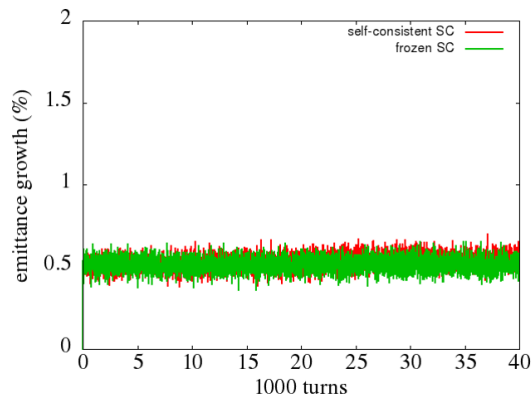


Figure 5: 4D emittance growth evolution with self-consistent simulation (red) and frozen space-charge model (green).

lution for the above example by using the self-consistent tracking and by using the frozen space-charge model. It is seen that the emittance growth evolution from the frozen space-charge model agrees with that from the self-consistent simulation quite well. The computational speed of the frozen space-charge model is about a factor of six faster than the self-consistent simulation in this case.

CONCLUSION

In this study, we suggested using a symplectic space-charge PIC model with threshold filtering in frequency domain of the charge density distribution to reduce the numerical artifacts in the simulation. By appropriately choosing threshold value, the numerical noise driven emittance growth can be significantly reduced in the long-term simulation. In order to improve the computing speed, we explored a frozen space-charge model that stores the space-charge field solutions after some initial steps and reuse those space-charge fields in the following long-term simulation. This method significantly reduces the computing time and yields reasonable simulation results in the above linear lattice example where the beam charge density distribution does vary much after 200 turns.

ACKNOWLEDGMENT

This research used computer resources at the National Energy Research Scientific Computing Center.

REFERENCES

- [1] A. Friedman, D. P. Grote, and I. Haber, *Phys. Fluids B* **4**, 2203 (1992).
- [2] H. Takeda and J. H. Billen, Recent developments of the accelerator design code PARMILA, in Proc. XIX International Linac Conference, Chicago, August 1998, p. 156.
- [3] S. Machida and M. Ikegami, in AIP Conf. Proc 448, p.73 (1998).
- [4] F. W. Jones and H. O. Schoenauer, Proc of PAC1999, p. 2933, 1999.
- [5] J. Qiang, R. D. Ryne, S. Habib, V. Decyk, *J. Comput. Phys.* **163**, 434, 2000.
- [6] P. N. Ostroumov and K. W. Shepard. *Phys. Rev. ST. Accel. Beams* **11**, 030101 (2001).
- [7] R. Duperrier, *Phys. Rev. ST Accel. Beams* **3**, 124201, 2000.
- [8] J. D. Galambos, S. Danilov, D. Jeon, J. A. Holmes, and D. K. Olsen, F. Neri and M. Plum, *Phys. Rev. ST Accel. Beams* **3**, 034201, (2000).
- [9] H. Qin, R. C. Davidson, W. W. Lee, and R. Kolesnikov, *Nucl. Instr. Meth. in Phys. Res. A* **464**, 477 (2001).
- [10] G. Franchetti, I. Hofmann, M. Giovannozzi, M. Martini, and E. Metral, *Phys. Rev. ST Accel. Beams* **6**, 124201, (2003).
- [11] J. Qiang, S. Lidia, R. D. Ryne, and C. Limborg-Deprey, *Phys. Rev. ST Accel. Beams* **9**, 044204, 2006.
- [12] J. Amundson, P. Spentzouris, J. Qiang and R. Ryne, *J. Comp. Phys.* vol. 211, 229 (2006).
- [13] http://amas.web.psi.ch/docs/opal/opal_user_guide.pdf
- [14] P. J. Channell and C. Scovel, *Nonlinearity* **3**, p.231 (1990).
- [15] T. J. Stuchi, *Brazilian J. Phys.* **32**, p. 958 (2002).
- [16] J. Qiang, *Phys. Rev. Accel. Beams* **20**, 014203, (2017).
- [17] J. Qiang, <https://arxiv.org/abs/1801.05288>
- [18] R.W. Hockney, J.W. Eastwood, *Computer Simulation Using Particles*, Adam Hilger, New York, 1988.
- [19] C. K. Birdsall and A. B. Langdon, *Plasma Physics Via Computer Simulation*, Taylor and Francis, New York, 2005.
- [20] <http://mad.web.cern.ch/mad/>.
- [21] R. D. Ryne, "Computational Methods in Accelerator Physics," US Particle Accelerator class note, 2012.
- [22] A. J. Dragt, "Lie Methods for Nonlinear Dynamics with Applications to Accelerator Physics," 2016.